

First experience with combined use of adaptive statistical iterative reconstruction and gemstone spectral imaging in spinal fusion CT images

Fengdan Wang, Yan Zhang, Zhengyu Jin, Richard Zwar

Objective. To explore whether the image noises and the metal artifacts could be further managed by the combined use of two technologies, the adaptive statistical iterative reconstruction (ASIR) and the monochromatic imaging generated by gemstone spectral imaging (GSI) dual-energy CT. **Materials and Methods.** Fifty-one patients with 318 spinal pedicle screws were prospectively scanned with dual energy CT by using fast kV-switching GSI between 80 and 140 kVp. The monochromatic GSI images at 110 keV were reconstructed either without ASIR or with ASIR of various levels (30%, 50%, 70% and 100%). For these five sets of images, both objective and subjective image quality assessments were performed to evaluate the image quality. **Results.** With objective image quality assessment, the metal artifacts (measured by an artifacts index) significantly decreased when increasing levels of ASIR was utilized ($p < 0.001$). Moreover, adding ASIR to GSI also decreased the image noise ($p < 0.001$) and improved the signal-to-noise ratio (SNR, $p < 0.001$). With subjective image quality analysis, the inter-reader agreements were good, with intra-class correlation coefficients (ICC) of 0.89 to 0.99. Meanwhile, the visualization of the peri-implant soft tissue was improved at higher ASIR levels ($p < 0.001$). **Conclusion.** Combined use of ASIR and GSI is shown to decrease the image noise and improve the image quality in post-spinal fusion CT scans. Optimal results were achieved with ASIR levels of over 70%.

**First experience with combined use of adaptive statistical iterative
reconstruction and gemstone spectral imaging in spinal fusion CT images**

This study was orally presented at the European Congress of Radiology of 2015.

Fengdan Wang^{1,a}, Yan Zhang^{1,a}, Zhengyu Jin¹, Richard Zwar²

¹Department of Radiology, Peking Union Medical College Hospital, Beijing, China

²Department of Radiology, Austin Health, Melbourne, Victoria, Australia

^aThese authors gave the same contribution to the paper and were recommended as first authors.

Corresponding author:

Zhengyu Jin¹

#1 Shuaifuyuan, Dongcheng District, Beijing, 100730, China.

Phone: +86-10-69159608

E-mail: pumchradiology@126.com

ABSTRACT

Objective. To explore whether the image noises and the metal artifacts could be further managed by the combined use of two technologies, the adaptive statistical iterative reconstruction (ASIR) and the monochromatic imaging generated by gemstone spectral imaging (GSI) dual-energy CT.

Materials and Methods. Fifty-one patients with 318 spinal pedicle screws were prospectively scanned with dual energy CT by using fast kV-switching GSI between 80 and 140 kVp. The monochromatic GSI images at 110 keV were reconstructed either without ASIR or with ASIR of various levels (30%, 50%, 70% and 100%). For these five sets of images, both objective and subjective image quality assessments were performed to evaluate the image quality.

Results. With objective image quality assessment, the metal artifacts (measured by an artifacts index) significantly decreased when increasing levels of ASIR was utilized ($p < 0.001$). Moreover, adding ASIR to GSI also decreased the image noise ($p < 0.001$) and improved the signal-to-noise ratio (SNR, $p < 0.001$). With subjective image quality analysis, the inter-reader agreements were good, with intra-class correlation coefficients (ICC) of 0.89 to 0.99. Meanwhile, the visualization of the peri-implant soft tissue was improved at higher ASIR levels ($p < 0.001$).

Conclusion. Combined use of ASIR and GSI is shown to decrease the image noise and improve the image quality in post-spinal fusion CT scans. Optimal results were achieved with ASIR levels of over 70%.

Keywords image noise, metal artifacts, dual-energy computed tomography, iterative reconstruction

INTRODUCTION

Spinal fusion surgery is a common treatment for spinal degenerative diseases, deformities, trauma, neoplastic and infectious diseases (*Manbachi, Cobbold & Ginsberg, 2014*). It is estimated that approximately 488,000 spinal fusions were performed in the USA annually (*Weiss, Elixhauser & Andrews, 2014*). Postoperative imaging evaluation is of critical importance to ensure the quality of surgery and rule out complications such as loosening of pedicle screws, malposition or fracture of metal implants, or infection at the surgery site (*Young et al., 2007*).

Compared to regular X-ray study, computed tomography (CT) is the preferred imaging modality for postoperative evaluation because of its multiplanar reformation capability, and detailed demonstration of hardware, grafts, and soft tissues (*Berlemann et al., 1997; Chrastil & Patel, 2012*). However, the quality of postoperative spinal CT images are often seriously impaired by two factors, the metal artifacts and the image noise, which make it difficult for the radiologists to evaluate the implants and the surrounding anatomic structures. Artifacts from metal implants are due to beam hardening and photon starvation (*Dinkel et al., 2015*), and can significantly reduce the readability of the CT image. Image noise is related to the radiation pattern and the processing software employed for generating the picture, and can seriously hampers the proper evaluation of soft tissue at the surgical site, which is of great clinical concern because most complications, especially postoperative infections, usually involve the soft tissue near the metal implants (*Chrastil & Patel, 2012*).

There are technologies developed to reduce the image artifacts from metal implants. Among the artifact-reducing approaches, monochromatic imaging generated by gemstone spectral imaging (GSI) dual-energy CT has been extensively studied and shown of value for effectively reducing metal artifacts (*Lee et al., 2012; Wang et al., 2013*). There are, however, limitations of images produced by GSI technology. GSI at high energy levels may increase the image noise and reduce the contrast to noise ratio (CNR), due to removal of the information generated by photons of low-energy levels (*Lewis, Reid & Toms, 2013*). Moreover, adopting GSI may increase the radiation exposure to the patients (*Venema, 2011*). As a result, it is necessary to develop new technologies that can further improve the GSI-based method for post-spinal fusion CT images.

Technologies have also been developed to reduce the CT image noise. Iterative reconstruction has been available since the advent of CT in the 1970s, but is only made practical in recent years due to the need of heavy computer processing power. By focusing on modeling of the scanned object and the noise properties, adaptive statistical iterative reconstruction (ASIR) is of benefit for those examinations that experience limitations due to noise in the reconstructed image, and can improve the diagnostic acceptability (*Marin et al., 2013; Singh et al., 2010*). Although GSI can reduce metal artifacts, it is also associated with increased image noise at high energy levels. Since the application of ASIR usually reduces image noise, the combinational use of GSI and ASIR may further improve the quality of CT images for evaluating post-spinal fusion

patients. However, prior studies about metal artifact reduction with GSI mainly focused on the application of GSI technology alone (*Lee et al., 2012; Wang et al., 2013*). We believe this study is the first to investigate the combined effectiveness of GSI and ASIR in post spinal fusion CT imaging.

In this study, we aim to evaluate the feasibility of using GSI and ASIR together in spinal fusion CT images. The hypothesis is that the combined use of GSI and ASIR will not only reduce the metal artifacts, but also lower the image noise that often hampers the proper evaluation of the soft tissues at the surgical site. The best ASIR setting for using with GSI was also explored.

MATERIALS AND METHODS

Patient population

This prospective study was fully approved by the institutional review board. The inclusion criteria were: 1) patients received spinal fusion surgery using pedicle screw implants made of titanium, 2) CT scans were clinically indicated for postoperative residual or recurrent pain, or before further surgery of adjacent segments, 3) informed consent was required. Patients were excluded if they were pregnant or lactating. All of the patients enrolled were prospectively scanned with GSI protocol.

CT scan protocol and reconstruction

Dual-energy CT was performed using a high definition 64-row detector Discovery CT750HD (GE Healthcare, Milwaukee, Wis, USA) with fast kV-switching between 80 kVp and 140 kVp. The detailed GSI parameters were set up by the manufacture as follows: tube current of 550mA, thickness of 0.625mm, pitch of 0.984:1, rotation time of 0.8s/rot, total exposure time of 6.2s, scanning field-of-view of large body, and displayed field-of-view of 18cm.

From the acquired data, monoenergetic images at 110 keV were reconstructed without ASIR (ASIR 0%) or with various blending levels of ASIR at 30%, 50%, 70%, and 100%. We chose the photon energy level of 110 keV to represent GSI images, as this level has been well demonstrated to be the most effective photon energy level to reduce metal artifacts by previous researches (*Meinel et al., 2012; Wang et al., 2013*). For every single patient, 5 sets of images were generated and transferred to a commercial workstation (GE VolumeShare ADW4.6, GE Healthcare). Bone window width was set at 2000 Hounsfield Unit (HU), and window level at 500HU. Soft tissue window width was set at 350HU, and window level at 40HU.

Objective image quality analysis

First, image noise and SNR were measured for every set of images. An oval region of interest (ROI) with 1.0×2.0cm was placed in subcutaneous fat without implants or artifacts. Its standard deviation (SD_f) of CT number was defined as the image noise. A similar ROI was drawn in

erector spinae muscle at the same level. SNR was calculated using the formula: $SNR = CT_m / SD_f$, where CT_m is the mean attenuation of the erector spinae muscle, and SD_f is the image noise.

Second, a well reported artifact index ($AI = \sqrt{SDa^2 - SDb^2}$) (Lin et al., 2011) was calculated to evaluate the severity of artifacts, where SDa represents the SD value in artifacts; SDb represents the SD value in the reference region free of artifacts. We further used AI_1 and AI_2 to stand for the hyperdense and hypodense artifacts respectively. All the ROIs were drawn carefully to cover most of the artifacts, and the exactly same ROIs were used in the reference images by using copy and paste function of the workstation.

Subjective image quality analysis

Two radiologists ([reader 1, R1] F.W. with 6 years of experience in general radiology, and [reader 2, R2] Y.Z. with 15 years of experience in musculoskeletal radiology), who were blinded to the imaging reconstruction method, independently read and scored the images by a 5-point Likert scale detailed in Table 1 (Guggenberger et al., 2012). The overall severity of artifacts of every set of images was analyzed and scored separately. Further assessment was made of the diagnostic quality of the images in visualization of implants, peri-implant bones and peri-implant soft tissues respectively.

Following induction as to the scoring system the two radiologists independently evaluated the images. Images were presented randomly on the workstations and three orthogonal plane reformats were available for assessment.

Table 1 Subjective image quality scoring system

Score	Artifacts	Visibility (implants, peri-implant bones and peri-implant soft tissues)
0	absence of artifacts	full visualization
1	minor streaks	good evaluation
2	mild artifacts	mildly affected
3	moderate artifacts	impaired evaluation
4	prominent artifacts	impossible evaluation

Statistical analysis

All variables are expressed as mean \pm standard deviation. The inter-reader agreements regarding the qualitative evaluations of R1 and R2 were analyzed using the intra-class correlation coefficients (ICC). ICC was defined as good (ICC = 0.61-0.8), and perfect agreement (ICC = 0.81-1.0). Because of the paired data, Wilcoxon signed ranks test was used for the qualitative variables, and paired student's t-test was used for the quantitative variables. Statistically significance was accepted as $p < 0.05$ for all comparisons. The statistical analysis was performed using SPSS software (version 18.0; IBM, Chicago, Ill, USA).

RESULTS

Study population

From September 2013 to March 2014, 51 patients with spinal fusion implants were prospectively scanned with GSI protocol in our medical center. The male to female ratio was 1.04:1. The mean age was 18.1 years (range, 5-83 years). These patients with a total of 318 pedicle screws underwent spine surgery for scoliosis, spinal stenosis, lumbar disk degeneration, spinal tumor, tuberculosis or trauma. The CT scan ranges were thoracic spine (1 patient), lumbar spine (41 patients), thoracic to lumbar spine (2 patients), and whole spine (7 patients). The average CT dose index (CTDI) was 23.56 mGy.

Objective image quality analysis

Images of patients with spinal prosthesis were assessed for artifact reduction with GSI technique either without ASIR or with varying levels of ASIR (30%, 50%, 70% and 100%). Typical results of images generated by ASIR combined with GSI were shown in Figure 1. The image quality of regular CT scan was significantly impaired by metal artifacts and noise. Compared with regular CT, GSI significantly reduced the metal artifacts. Adding ASIR to GSI further reduced the image noise in soft tissue, while retaining the effects of metal artifact reduction by GSI. The results suggested that the combinational use of GSI and ASIR could not only reduce the artifacts from metal implant, but also lower the image noises.

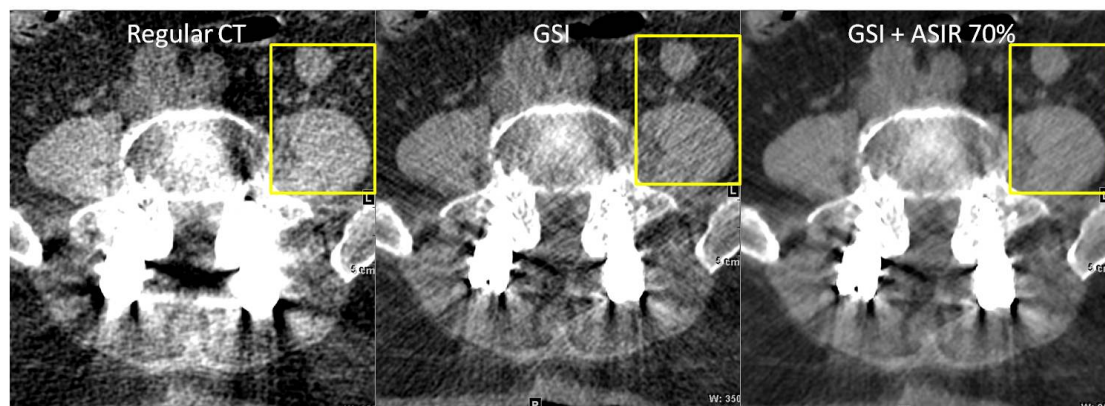


Figure 1 Comparison of CT images generated by different reconstruction algorithms for evaluation of a 65-year-old female with lumbar internal fixation for spinal stenosis. Regular CT scan (left image) was plagued with metal artifacts and image noises. GSI technique (center image) significantly reduced the metal artifacts, but still had obvious image noise in soft tissues. The combined use of GSI and ASIR (right image) not only reduced the metal artifacts, but also significantly lowered the image noise of soft tissues (illustrated by the muscle and small bowel within the rectangular boxes).

To further validate the effects on image quality by various CT processing algorithms, quantitative evaluation of CT images was also performed. As shown in Figure 2, there was a trend for decreasing image noise with the application of ASIR. Specifically, the image noise was

significantly decreased by 45%, from 13.66 ± 2.73 HU without ASIR to 7.40 ± 2.51 HU at ASIR of 100% ($p < 0.001$, Fig. 2A). This was accompanied by an almost doubled signal-to-noise ratio (SNR), from 3.04 ± 1.08 without ASIR to 5.85 ± 2.47 at ASIR of 100% ($p < 0.001$, Fig. 2B). These results again suggested that the quality of CT image generated by GSI could be further improved by application of ASIR.

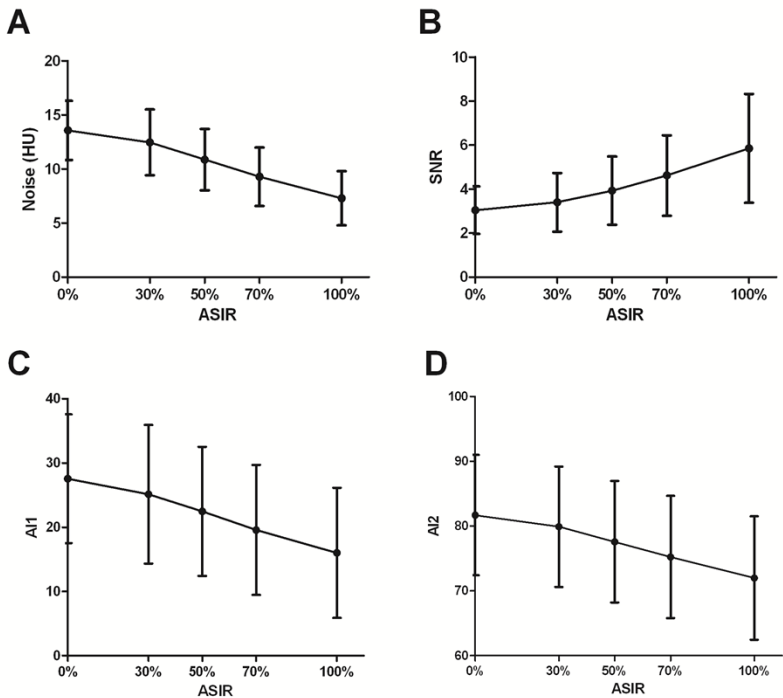


Figure 2 Quantitative image quality assessments at various ASIR levels. As the level of ASIR increased, image noise (A) decreased, and the SNR (B) substantially increased. Both AI of hyperdense artifacts (C) and AI of hypodense artifacts (D) were decreased with increasing levels of ASIR.

Additionally, the artifact index (AI) and the standard deviation (SD) values of both hyperdense and hypodense artifacts were also calculated, in order to objectively assess the metal artifacts in CT images generated by various algorithms (Table 2, Figs. 2C and 2D). As the ASIR level increased, the SD values of hyperdense artifacts dropped from 32.99 ± 8.31 HU at ASIR of 0% to 20.57 ± 8.29 HU at ASIR of 100%. Similarly, the SD values of hypodense artifacts decreased from 84.08 ± 66.07 HU at ASIR of 0% to 73.32 ± 67.95 HU at ASIR of 100% (Table 2). Moreover, increasing levels of ASIR also significantly reduced the AIs of both the hyperdense and the hypodense artifacts (Figs. 2C and 2D, $p < 0.001$). These results indicated that adding ASIR to GSI did not impair the artifacts reduction capability of GSI processing.

Table 2 SD and AI values of hyperdense and hypodense artifacts at various levels of ASIR

Parameter	ASIR 0%	ASIR 30%	ASIR 50%	ASIR 70%	ASIR 100%	P value
SDa ₁	32.99±8.31	30.94±8.09	27.60±8.08	24.42±8.25	20.57±8.29	
SDb ₁	16.82±4.09	16.20±5.00	14.38±4.60	12.95±4.64	11.07±4.65	

AI ₁	27.54±10.04	25.12±10.79	22.46±10.04	19.57±10.12	16.00±10.14	< 0.001
SDa ₂	84.08±66.07	82.12±66.12	79.47±66.70	76.86±67.20	73.32±67.95	
SDB ₂	18.07±6.17	16.92±6.28	15.22±6.19	13.82±6.07	11.88±5.95	
AI ₂	81.68±66.33	79.92±66.36	77.58±66.91	75.22±63.37	71.99±66.09	< 0.001

Results are shown as mean ± standard deviation. *P* represents the probability of equivalence. SD stands for standard deviation. AI₁ and AI₂ stand for artifact index of hyperdense and hypodense artifacts, respectively. SDa₁ and SDb₁ represent the SD values of hyperdense artifacts and the reference site, respectively. SDa₂ and SDb₂ represent the SD values of hypodense artifacts and the reference site, respectively.

Subjective image quality analysis

Since the subject judgments of different radiologist may affect the proper interpretation of CT images, it is also important to perform a subjective image quality analysis that involves more than one radiologist. Because most postoperative problems are related with the metal implants and the adjacent structures, subjective assessments of diagnostic quality in regard to implant and peri-implant bone and soft tissues were performed separately for every blending level of ASIR shown in Figure 3 separately by two radiologists (R1 and R2). The results (Table 3) demonstrated excellent inter-reader agreements for the assessments of artifacts (ICC = 0.92), implants (ICC = 0.99), adjacent bone (ICC = 0.89) and adjacent soft tissue (ICC = 0.93). As illustrated in Figure 4, for both readers, the scores of artifacts decreased when ASIR level increased to 70% or more ($p < 0.001$). For R1, the visualization of adjacent soft tissue was improved with ASIR levels of 70% and 100% ($p < 0.05$); whereas for R2, it was improved with ASIR level of 100% ($P = 0.014$). Regarding the implants and adjacent bones, the scores did not change significantly even when ASIR level increased to 100% (all $p > 0.05$). The results suggested that higher levels of ASIR (70% and above) could improve the diagnostic quality in regard to soft tissue visualization, but made less impact on visualization of implants and adjacent bone.

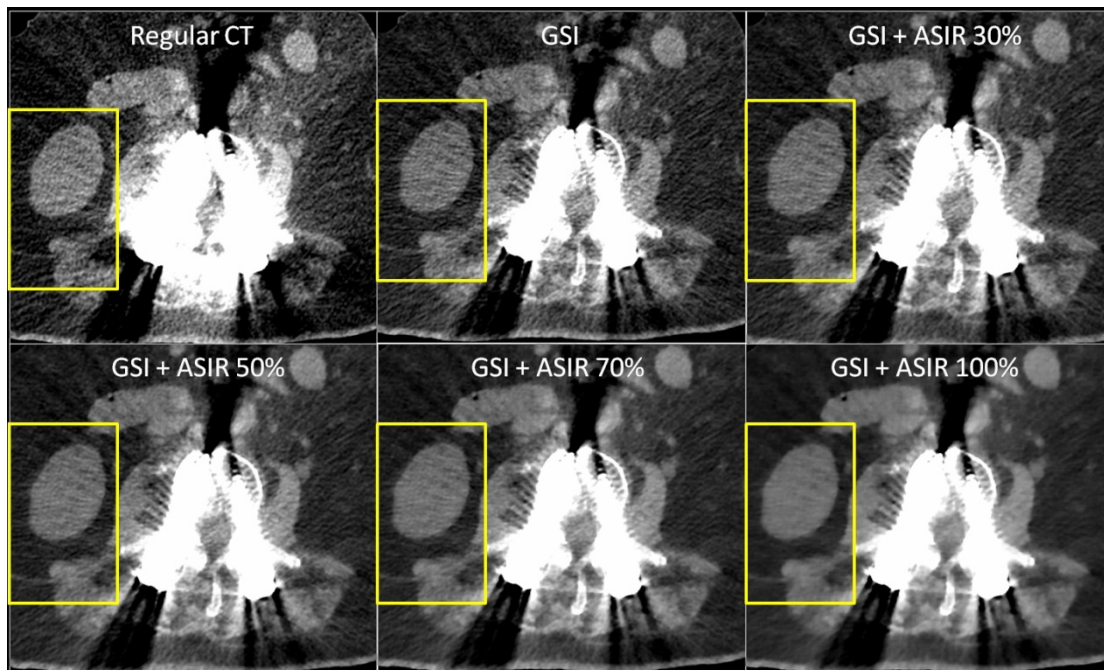


Figure 3 Effects of various blending levels of ASIR with GSI for evaluation of a 60-year-old male with lumbar internal fixation for disk herniation. The screws generated remarkable metal artifacts in regular CT, which were significantly reduced by the GSI technique. However, the GSI scan still had noisy soft tissue images (indicated by the right kidney and surrounding muscles within the rectangle box). By adding increasing levels of ASIR to GSI, image noise was gradually reduced, and the appearance of tissue structure became smoother. Please note that all CT images were reconstructed from one GSI scan.

Table 3 Scores of artifact severity and visualization of implants and adjacent structures at various ASIR levels

Parameter	Rater	ICC	0%	30%	50%	70%	100%	<i>P</i> value
artifacts	R1	0.92	3.20±0.53	3.18±0.56	3.16±0.54	2.41±0.61§	2.22±0.54§	< 0.001
	R2		2.53±0.50	2.53±0.50	2.53±0.50	2.10±0.81§	1.63±0.60§	< 0.001
implants	R1	0.99	1.78±0.46	1.78±0.46	1.78±0.46	1.78±0.46	1.77±0.47	> 0.05
	R2		1.78±0.46	1.78±0.46	1.78±0.46	1.78±0.46	1.78±0.46	> 0.99
bone	R1	0.89	1.96±0.28	1.96±0.28	1.96±0.28	1.96±0.28	1.96±0.28	> 0.99
	R2		2.00±0.00	2.00±0.00	2.00±0.00	2.00±0.00	2.00±0.00	> 0.99
soft tissue	R1	0.93	2.41±0.54	2.41±0.54	2.41±0.54	2.26±0.52†	2.24±0.55†	< 0.05
	R2		2.53±0.50	2.53±0.50	2.53±0.50	2.49±0.58	2.41±0.61†	< 0.05

Results are shown as rating ± standard deviation. *P* represents the probability of equivalence. ICC stands for intra-class correlation coefficient. R1 and R2 stand for reader 1 and reader 2, respectively. § *P* < 0.001 compared with GSI images without ASIR. † *P* < 0.05 compared with GSI images without ASIR.

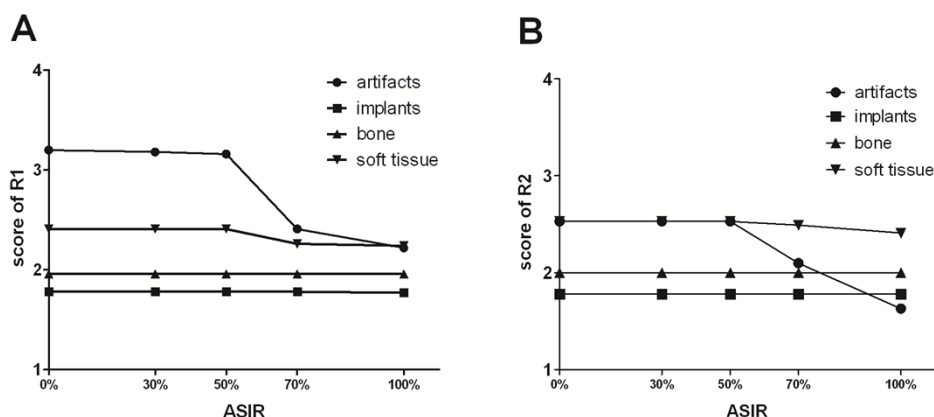


Figure 4 Subjective image quality assessments by two radiologists (image readers). For both reader 1 (A) and reader 2 (B), the scores of artifacts were decreased with 70% and 100% ASIR levels. The visualization of soft tissue showed a mild improvement at ASIR levels of 70% and above. However, the scores of implants and adjacent bones didn't change significantly.

DISCUSSION

CT assessment of spinal metal implants and adjacent tissues postoperatively is often seriously impaired by metal artifacts and image noise. We present a study of 51 post-spinal fusion patients with 318 pedicle screws using both GSI and ASIR techniques for postoperative CT evaluation. To our knowledge this is the first study to report this combination of techniques for such a patient group. We found that by adding ASIR to GSI images, image noise and SNR were markedly improved (Figs. 1 and 2). Moreover, both hyperdense and hypodense artifacts index were decreased with increased contributions of ASIR (Table 2 and Fig. 2). This effect was confirmed by subjective assessment at ASIR levels of 70% or higher (Table 3, Figs. 3 and 4). The visualization of adjacent soft tissue was also improved at high levels of ASIR. These results indicate that a combination of ASIR and GSI may reduce image noise and provide better image quality in postoperative CT evaluation of spinal fusion patients.

Monochromatic images generated from GSI dual-energy CT could avoid the shortcoming of polychromatic X-ray beams by reducing metal artifacts from energy averaging. This method has previously been demonstrated to reduce metal artifacts from internal fixation, spinal screws and large hip prostheses (Wang, et al. 2013; Wang et al., 2014). Photon energy level of 110 keV was recommended to provide the optimal metal artifacts reduction effect by GSI. However, it has also been shown that the increasing photon energy level may cause increased background heterogeneity and noise (Lewis, Reid & Toms, 2013). ASIR was proven by our study to be an effective tool to overcome this drawback of GSI imaging.

In order to further reduce metal artifacts, many attempts have also been devoted to metal

artifact reduction algorithms based on an inpainting method, such as metal artifact reduction software (MARS) in GE, metal artifact reduction for orthopedic implants (O-MAR) in Phillips, single-energy metal artifact reduction (SEMAR) in Toshiba, and iterative metal artifact reduction (iMAR) in Siemens. It has been well investigated that MARS combined with GSI could effectively reduce metal artifacts in pinnings, shoulder and hip prostheses ([Lee et al., 2012](#); [Wang et al., 2014](#)). Nevertheless, from both literature and our own experiences, this combinational use does not work well for relatively thin and small spinal screws made of titanium, because MARS probably will cause implants distortion, introduce new artifacts and blur the surroundings soft tissues ([Wang et al., 2013](#); [Watzke & Kalender, 2004](#)). So in this study, we only investigated ASIR implanted to GSI without MARS to study the image quality.

Iterative reconstruction introduces a loop of image correction by feeding through the entire synthesizing and updating process to obtain a newly updated image ([Sagara et al., 2010](#); [Wang et al., 2012](#)), and therefore enables a significant reduction in image noise. The combined use of GSI and ASIR has been investigated recently in coronary computed tomography angiography ([Fuchs et al., 2013](#)), where noise reduction occurs with increasing contributions of ASIR. To date, however, this combination of GSI and ASIR has not been reported in post spinal fusion CT images. The current study served as the first experience of using the two methods together in metal artifacts reduction for spinal fusion patients. Our results also indicated that increasing ASIR could reduce the image noise of GSI imaging by up to 45%, and generate an almost 2-fold increase of SNR.

Moreover, iterative reconstruction processing has been implanted into several algorithms for metal artifact reduction ([Boas & Fleischmann, 2011](#); [Dong, Hayakawa & Kober, 2014](#); [Morsbach et al., 2013a](#)), but iterative reconstruction itself might have limited metal artifact reduction ability. In our study, though the artifact index of both hyperdense and hypodense artifacts gradually decreased with the increasing blending levels of ASIR during the quantitative evaluation, the changes of artifacts score for both readers were less than 1 grade even when ASIR was added up to 100%. We also noticed that the characteristics of artifact index curves were very similar to that of image noise curve illustrated in [Figure 2](#). Therefore, the minor artifact reduction effect of ASIR might be the result of remarkable reduction of image noise ([Morsbach et al., 2013b](#)). Nevertheless, ASIR combined with GSI could have comparable artifacts reduction ability with GSI, resulting in better visualization of the adjacent soft tissue.

The findings that ASIR could further improve image quality of GSI imaging may have some clinical implications. In one way, with the same radiation dose of GSI scanning, better image quality could be achieved by the combined usage of ASIR and GSI. In another way, ASIR may have the potential to reduce radiation dose. Nowadays, the radiation dose of CT and its associated risks are major concerns for doctors and patients ([Albert, 2013](#)). As such, the dose must be rendered as low as possible. There has been concern that GSI may hold higher radiation dose compared to standard CT imaging ([Venema, 2011](#)). The tuber current of 550mA used in

GSI scan is higher than that of around 350mA used in most regular lumbar non-GSI scanners, which may result in additional radiation dose. However, with the application of iterative reconstruction, the same noise and SNR may be achieved with lower dose of radiation (*Hwang et al., 2012; Marin et al., 2010*).

Admittedly, there are several limitations of our study. Firstly, all of the implants used in the spinal fusion surgery in our medical center are made of titanium. Further investigation of the combined use of ASIR and GSI would be valuable to assess orthopedic implants other than titanium spinal hardware. Secondly, as only the photon energy of 110 keV was used in this study, future research could evaluate different photon energy levels when ASIR is applied. Thirdly, higher level of iterative reconstruction may generate plastic-like images, but image appearance was not assessed in our study for our purpose mainly focused on image noise and metal artifacts.

CONCLUSION

Combinational usage of ASIR and GSI could reduce image noise and improve image quality of spinal fusion CT images, with higher ASIR ($\geq 70\%$) used to achieve optimal image quality.

ACKNOWLEDGEMENTS

The authors thank Dr Huadan Xue, Dr Shugang Li, Dr Zhihong Wu and Prof Xianda Yang for their generous help and guidance. We also thank Bing Qi and Suo Ma for their technical support.

CONFLICTS OF INTEREST

None declared.

REFERENCES

Albert JM. 2013. Radiation risk from CT: implications for cancer screening. *American Journal of Roentgenology* **201**:W81-W87 DOI [10.2214/AJR.12.9226](https://doi.org/10.2214/AJR.12.9226).

Berlemann U, Heini P, Muller U, Stoupis C, Schwarzenbach O. 1997. Reliability of pedicle screw assessment utilizing plain radiographs versus CT reconstruction. *European Spine Journal* **6**:406-410 DOI [10.1007/BF01834069](https://doi.org/10.1007/BF01834069).

Boas FE, Fleischmann D. 2011. Evaluation of two iterative techniques for reducing metal artifacts in computed tomography. *Radiology* **259**:894-902 DOI [10.1148/radiol.11101782](https://doi.org/10.1148/radiol.11101782).

Chrastil J, Patel AA. 2012. Complications associated with posterior and transforaminal lumbar interbody fusion. *Journal of the American Academy of Orthopaedic Surgeons* **20**:283-291 DOI [10.1148/radiol.11101782](https://doi.org/10.1148/radiol.11101782).

Dinkel J, Khalilzadeh O, Phan CM, Goenka AH, Yoo AJ, Hirsch JA, Gupta R. 2015. Technical limitations of dual-energy CT in neuroradiology: 30-month institutional experience and review of literature. *Journal of Neurointerventional Surgery* **7**:596-602 DOI [10.1136/neurintsurg-2014-011241](https://doi.org/10.1136/neurintsurg-2014-011241).

Dong J, Hayakawa Y, Kober C. 2014. Statistical iterative reconstruction for streak artefact reduction when using

multidetector CT to image the dento-alveolar structures. *Dentomaxillofacial Radiology* **43**:20130373 DOI [10.1259/dmfr.20130373](https://doi.org/10.1259/dmfr.20130373).

Fuchs TA, Stehli J, Fiechter M, Dougoud S, Gebhard C, Ghadri JR, Husmann L, Gaemperli O, Kaufmann PA. 2013. First experience with monochromatic coronary computed tomography angiography from a 64-slice CT scanner with Gemstone Spectral Imaging (GSI). *Journal of Cardiovascular Computed Tomography* **7**:25-31 DOI [10.1016/j.jcct.2013.01.004](https://doi.org/10.1016/j.jcct.2013.01.004).

Guggenberger R, Winklhofer S, Osterhoff G, Wanner GA, Fortunati M, Andreisek G, Alkadhi H, Stolzmann P. 2012. Metallic artefact reduction with monoenergetic dual-energy CT: systematic ex vivo evaluation of posterior spinal fusion implants from various vendors and different spine levels. *European Radiology* **22**:2357-2364 DOI [10.1007/s00330-011-2370-5](https://doi.org/10.1007/s00330-011-2370-5).

Hwang HJ, Seo JB, Lee JS, Song JW, Kim SS, Lee HJ, Lim CH. 2012. Radiation dose reduction of chest CT with iterative reconstruction in image space - Part I: studies on image quality using dual source CT. *Korean Journal of Radiology* **13**:711-719 DOI [10.3348/kjr.2012.13.6.711](https://doi.org/10.3348/kjr.2012.13.6.711).

Lee YH, Park KK, Song HT, Kim S, Suh JS. 2012. Metal artefact reduction in gemstone spectral imaging dual-energy CT with and without metal artefact reduction software. *European Radiology* **22**:1331-1340 DOI [10.1007/s00330-011-2370-5](https://doi.org/10.1007/s00330-011-2370-5).

Lewis M, Reid K, Toms AP. 2013. Reducing the effects of metal artefact using high keV monoenergetic reconstruction of dual energy CT (DECT) in hip replacements. *Skeletal Radiology* **42**:275-282 DOI [10.1007/s00256-012-1458-6](https://doi.org/10.1007/s00256-012-1458-6).

Lin XZ, Miao F, Li JY, Dong HP, Shen Y, Chen KM. 2011. High-definition CT Gemstone spectral imaging of the brain: initial results of selecting optimal monochromatic image for beam-hardening artifacts and image noise reduction. *Journal of Computer Assisted Tomography* **35**:294-297 DOI [10.1097/RCT.0b013e3182058d5c](https://doi.org/10.1097/RCT.0b013e3182058d5c).

Manbachi A, Cobbold RS, Ginsberg HJ. 2014. Guided pedicle screw insertion: techniques and training. *The Spine Journal* **14**:165-179 DOI [10.1016/j.spinee.2013.03.029](https://doi.org/10.1016/j.spinee.2013.03.029).

Marin D, Choudhury KR, Gupta RT, Ho LM, Allen BC, Schindera ST, Colsher JG, Samei E, Nelson RC. 2013. Clinical impact of an adaptive statistical iterative reconstruction algorithm for detection of hypervascular liver tumours using a low tube voltage, high tube current MDCT technique. *European Radiology* **23**:3325-3335 DOI [10.1007/s00330-013-2964-1](https://doi.org/10.1007/s00330-013-2964-1).

Marin D, Nelson RC, Schindera ST, Richard S, Youngblood RS, Yoshizumi TT, Samei E. 2010. Low-tube-voltage, high-tube-current multidetector abdominal CT: improved image quality and decreased radiation dose with adaptive statistical iterative reconstruction algorithm--initial clinical experience. *Radiology* **254**:145-153 DOI [10.1148/radiol.09090094](https://doi.org/10.1148/radiol.09090094).

Meinel FG, Bischoff B, Zhang Q, Bamberg F, Reiser MF, Johnson TR. 2012. Metal artifact reduction by dual-energy computed tomography using energetic extrapolation: a systematically optimized protocol. *Investigative Radiology* **47**:406-414 DOI [10.1097/RLI.0b013e31824c86a3](https://doi.org/10.1097/RLI.0b013e31824c86a3).

Morsbach F, Bickelhaupt S, Wanner GA, Krauss A, Schmidt B, Alkadhi H. 2013a. Reduction of Metal Artifacts from Hip Prostheses on CT Images of the Pelvis: Value of Iterative Reconstructions. *Radiology* **268**:237-244 DOI [10.1148/radiol.13122089](https://doi.org/10.1148/radiol.13122089).

Morsbach F, Wurnig M, Kunz DM, Krauss A, Schmidt B, Kollias SS, Alkadhi H. 2013b. Metal artefact reduction from dental hardware in carotid CT angiography using iterative reconstructions. *European Radiology* **23**:2687-2694 DOI [10.1007/s00330-013-2885-z](https://doi.org/10.1007/s00330-013-2885-z).

- Sagara Y, Hara AK, Pavlicek W, Silva AC, Paden RG, Wu Q. 2010.** Abdominal CT: comparison of low-dose CT with adaptive statistical iterative reconstruction and routine-dose CT with filtered back projection in 53 patients. *American Journal of Roentgenology* **195**:713-719 DOI 10.2214/AJR.09.2989.
- Singh S, Kalra MK, Hsieh J, Licato PE, Do S, Pien HH, Blake MA. 2010.** Abdominal CT: comparison of adaptive statistical iterative and filtered back projection reconstruction techniques. *Radiology* **257**:373-383 DOI 10.1148/radiol.10092212.
- Venema HW. 2011.** Virtual monochromatic spectral imaging with fast kilovoltage switching should not be used as standard CT imaging modality. *Radiology* **260**:916-917 DOI 10.1148/radiol.11110654.
- Wang F, Xue H, Yang X, Han W, Qi B, Fan Y, Qian W, Wu Z, Zhang Y, Jin Z. 2014.** Reduction of metal artifacts from alloy hip prostheses in computer tomography. *Journal of Computed Assisted Tomography* **38**:828-833 DOI 10.1097/RCT.000000000000125.
- Wang R, Yu W, Wu R, Yang H, Lu D, Liu J, Zhang Z, Zhang C. 2012.** Improved image quality in dual-energy abdominal CT: comparison of iterative reconstruction in image space and filtered back projection reconstruction. *American Journal of Roentgenology* **199**:402-406 DOI 10.2214/AJR.11.7159.
- Wang Y, Qian B, Li B, Qin G, Zhou Z, Qiu Y, Sun X, Zhu B. 2013.** Metal artifacts reduction using monochromatic images from spectral CT: Evaluation of pedicle screws in patients with scoliosis. *European Journal of Radiology* **82**:e360-e366 DOI 10.1016/j.ejrad.2013.02.024.
- Watzke O, Kalender WA. 2004.** A pragmatic approach to metal artifact reduction in CT: merging of metal artifact reduced images. *European Radiology* **14**:849-856 DOI 10.1007/s00330-004-2263-y.
- Weiss AJ, Elixhauser A, Andrews RM. 2014.** Characteristics of Operating Room Procedures in U.S. Hospitals, 2011: Statistical Brief #170. Available at <https://www.hcup-us.ahrq.gov/reports/statbriefs/sb170-Operating-Room-Procedures-United-States-2011.jsp>.
- Young PM, Berquist TH, Bancroft LW, Peterson JJ. 2007.** Complications of spinal instrumentation. *Radiographics* **27**:775-789 DOI 10.1148/rg.273065055.